

Dawn Mission to Vesta and Ceres

Symbiosis between Terrestrial Observations and Robotic Exploration

C. T. Russell · F. Capaccioni · A. Coradini · M. C. De Sanctis ·
W. C. Feldman · R. Jaumann · H. U. Keller · T. B. McCord ·
L. A. McFadden · S. Mottola · C. M. Pieters · T. H. Prettyman ·
C. A. Raymond · M. V. Sykes · D. E. Smith · M. T. Zuber

Received: 21 August 2007 / Accepted: 22 August 2007 / Published online: 14 September 2007
© Springer Science+Business Media B.V. 2007

Abstract The initial exploration of any planetary object requires a careful mission design guided by our knowledge of that object as gained by terrestrial observers. This process is very evident in the development of the Dawn mission to the minor planets 1 Ceres and 4 Vesta. This mission was designed to verify the basaltic nature of Vesta inferred both from its reflectance spectrum and from the composition of the howardite, eucrite and diogenite meteorites believed to have originated on Vesta. Hubble Space Telescope observations have determined Vesta's size and shape, which, together with masses inferred from gravitational perturbations, have provided estimates of its density. These investigations have enabled the Dawn team to choose the appropriate instrumentation and to design its orbital operations at Vesta. Until recently Ceres has remained more of an enigma. Adaptive-optics and HST observations now have provided data from which we can begin

C. T. Russell (✉)
IGPP & ESS, UCLA, Los Angeles, CA 90095-1567, USA
e-mail: ctrussel@igpp.ucla.edu

F. Capaccioni
INAF, Via del fosso del Cavaliere, Rome 00133, Italy

A. Coradini
IFSI, Via del fosso del Cavaliere, Rome 00133, Italy

M. C. De Sanctis
IAFS, Via del fosso del Cavaliere, Rome 00133, Italy

W. C. Feldman · T. H. Prettyman
LANL, MS D466, NIS-1, Los Alamos, NM 87545, USA

R. Jaumann · S. Mottola
DLR Rutherfordstr 2, 12489 Berlin, Germany

H. U. Keller
MPAE, 37191 Katlenburg-Lindau, Germany

T. B. McCord
University of Hawaii, 2525 Correa Rd., Honolulu, HI 96822, USA

to confidently plan the mission. These observations reveal a rotationally symmetric body with little surface relief, an ultraviolet bright point that can be used as a control point for determining the pole and anchoring a geographic coordinate system. They also reveal albedo and color variations that provide tantalizing hints of surface processes.

Keywords Dawn Discovery mission · Asteroids · Ceres · Vesta

1 Introduction

The solar system is thought to have arisen from a cold cloud of gas and dust such as that observed in the Trifid nebula in which stars are being formed today. These young stars are bright UV emitters that heat the region around them. Eventually they prevent further precipitation of planetary materials from the surrounding nebula as the gas is dissipated. The conditions in such a nebula during this early evolutionary phase have been captured by the W. B. Hartmann painting shown in Fig. 1. This picture has served as an inspiration for the Dawn mission whose objective is to learn as much as possible about the formative stage of the solar system by visiting the two most massive bodies that have survived intact, the minor planets 1 Ceres and 4 Vesta.

As depicted in Fig. 1 the solar system formed from the gas and dust by accreting small bodies that in turn collided to form yet larger bodies, leading eventually to what one could term planetary embryos and protoplanets. This evolutionary sequence is illustrated in Fig. 2. The embryos grow during a period of about 3 million years and the terrestrial planets in about 30 million years (Jacobsen 2003). At 1 Astronomical Unit (AU), it is believed that the Earth underwent one last giant collision with a Mars-size protoplanet that resulted in the early Earth and a ring of material that coalesced to form the Moon.

The gravitational energy released when bodies collide with terrestrial-size planets is sufficient to cause complete melting, but collisions of small bodies of the size of planetary embryos will not result in melting throughout by gravitational energy alone. Thus an additional heat source would be necessary if the small embryos were to evolve through melting. A possible heat source is ^{26}Al , whose decay products have been found in meteorites. Since ^{26}Al has a very short half-life, it would have had to be produced close to the

L. A. McFadden
University of Maryland, College Park, MD 20742, USA

C. M. Pieters
Brown University, Providence, RI 02912, USA

C. A. Raymond
JPL, 4800 Oak Grove Dr, Pasadena, CA 91109, USA

M. V. Sykes
PSI, 1700 East Fort Lowell, Suite 106, Tucson, AZ 85719-2395, USA

D. E. Smith
GSFC, MC 920, Greenbelt, MD 20771, USA

M. T. Zuber
MIT, Cambridge, MA 02139, USA



Fig. 1 Painting of the conditions expected in the early solar nebula. (W. B. Hartmann, with permission). See TBD for color version

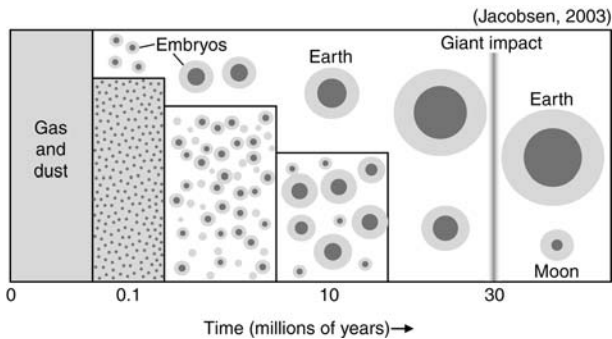


Fig. 2 Time scales for solar system formation (after Jacobsen 2003)

beginning of solar system formation, perhaps by a supernova. Thus both the timing of any such supernova and the timescale for assembly of the planetary embryos is critical to the ultimate evolution of the early minor planets and their precursors.

1 Ceres, 2 Pallas and 4 Vesta are the three largest minor planets, apparently intact survivors from the earliest period of the formation of the solar system. The surfaces of Ceres and Pallas are difficult to interpret in terms of composition from their reflectance spectra. Definitive absorption bands are lacking in the visible (Gaffey and McCord 1978) while the infrared spectrum of Ceres shows evidence for structural water in clay minerals (Lebofsky et al. 1981). Vesta, on the other hand, has a spectral reflectance signature of basaltic magma indicating extensive melting and thermal evolution (McCord et al. 1970). The reflectance spectrum of Vesta resembles greatly that of a class of meteorites, the howardites, eucrites and diogenites or HED meteorites. This association, that is now widely accepted, in turn allows us to infer much about the evolution and present day structure of Vesta. Metal segregation and core formation is suggested by the depletion of siderophile elements in HED meteorites (Ni, Co, Mo, W, P) relative to the non-siderophile elements (e.g., Hewins and Newson, 1988; Righter and Drake 1996). From this depletion modest core sizes have been estimated with masses up to 25% of the total mass of the asteroid (Dreibus et al. 1997; Ruzicka et al. 1997; Righter and Drake 1997).

In contrast Ceres, a much larger minor planet, does not have a surface with basaltic composition, nor is there a body of meteoritic evidence that provides insights into its thermal evolution. Ceres has kept its secrets hidden much more completely than has Vesta. It is necessary to go to Ceres to obtain even the most basic information. At the same time we must continue to try to learn as much as we can about Ceres in order to plan that in situ investigation.

In designing a planetary mission it rapidly becomes evident that much more can be learned with an orbiter than with a flyby mission. However, with a standard chemically fueled engine it is difficult within the cost cap of a small mission program such as Discovery to do anything but to fly by. One cannot build or launch a large enough spacecraft within the cost cap to carry the chemical fuel needed to get into orbit. A fortunate recent development is the qualification of ion engines for deep space use by the technology validation, Deep Space 1 (DS1) mission which was launched in 1998. Ion engines use an inert gas, xenon, as fuel, ionizing it, and accelerating it electrostatically at velocities of up to 31 km/s, about 10 times faster than the fuel expelled in a chemical rocket. Thus 10 times the change in momentum is possible per unit mass of fuel using electric propulsion. This efficiency in the use of fuel enables a spacecraft to be launched on a modestly-sized rocket such as a Delta II to spiral out from 1 AU to say 3 AU, slow down, and enter orbit with no chemical propulsion except that of the original launch vehicle at Earth. Eventually when the mapping of the planet is complete, the ion engines can be used to leave the body and if enough fuel remains, to go to another body, as is planned for Dawn.

As noted above the three key asteroids for exploring the state of the early solar system are Ceres, Pallas and Vesta because they appear to be intact survivors of the early solar system. Ceres has an average semi-major axis of 2.77 AU and has an inclination to the ecliptic plane of 10.6° . Vesta is closer to the Sun at 2.36 AU and at an inclination of 7.1° . Pallas, on the other hand, is at 2.77 AU and an inclination of 34.8° . This high inclination makes a Pallas mission very difficult, even with ion propulsion. In contrast it is possible to design an ion propulsion mission to visit and orbit both Vesta and Ceres with a modest fuel load. That is what the Dawn mission proposed to do and in December 2001, it was selected by NASA for development.

Dawn represents a major step over the earlier Discovery mission, NEAR, that orbited Eros. Figure 3 shows to scale images of the three asteroids, Eros, Vesta and Ceres. The average radius of Eros is 8.3 km, that of Vesta 258 km, and that of Ceres 470 km. Vesta

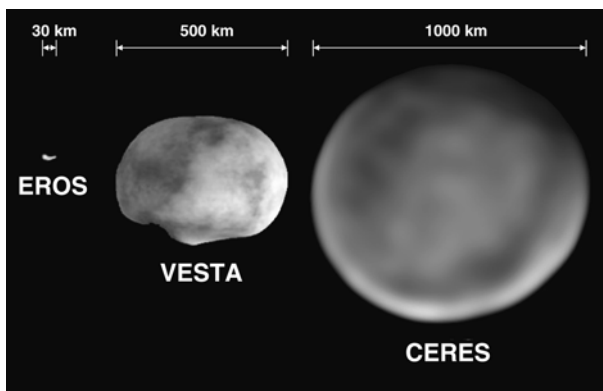


Fig. 3 Images of Eros, Vesta and Ceres to scale

and Ceres are more akin to the Earth and Mars than they are to Eros. Nevertheless, we use a similar payload to that of the NEAR mission because our goals of characterizing the surface and the interior are similar.

In this paper we wish to describe the history leading up to the development of the Dawn mission, what we know about Vesta and Ceres illustrating the synergy between observations at 1 AU and the design of a mission, and the present status and plans for the mission. First, of interest to anyone who might be contemplating leading a Discovery mission, we briefly describe the extended effort leading to selection and confirmation. Those interested solely in the science of the mission can skip ahead to the discussion on our knowledge of Vesta and Ceres followed by a discussion of the payload, mission design and operations. Throughout we describe the influence of 1 AU observations on our understanding of these bodies and ultimately on the design of the mission.

2 Dawn's Early History

The Discovery program began in the early 1990's with the selection of two non-PI-led missions, NEAR and Mars Pathfinder to be developed at a cost of under \$150M. In order to evolve the program into PI-led missions a community workshop was held where mission concepts were exposed with the goal of selecting some for further study with NASA funds. At this workshop one of the proposed concepts was to use an ion engine to make measurements in the Earth's magnetosphere. This seemed inappropriate for a planetary opportunity, but one of the authors, C. T. Russell, who attended the workshop recognized the advantages of ion propulsion for planetary exploration and joined forces with the NASA Lewis Research Center (now NASA Glenn RC) to explore possible planetary missions using this new capability. When the first opportunity to propose a PI-led mission was announced, a team allied with NASA Lewis and JPL was ready and in 1994 proposed an ambitious two-body mission, Diana, to explore the Moon and then a near-Earth asteroid/dormant comet, Wilson-Harrington. Instead of Diana, the first selections went to Lunar Prospector, an inexpensive, more traditional lunar mission, and Stardust, a comet-flyby, dust-sampling mission. The team was disappointed by this turn of events but undeterred.

In the opinion of the team the next two highest priority missions were to rendezvous with a comet and to explore the main asteroid belt, both of which were possible with ion propulsion. Not being able to decide between them the team submitted two proposals in 1996, one to fly to comet Tempel 2 and orbit it (Comet Nucleus Rendezvous) and one to fly to Vesta and two smaller asteroids, 857 Glasenappia and 21 Lutetia and orbit successively all three (Main Belt Asteroid Rendezvous). Again neither ion propulsion mission was selected. Instead Genesis, a mission to gather solar wind samples was selected, as well as a comet nucleus tour (CONTOUR) mission to fly by three comets.

The next proposal opportunity came in 1998. By this time ESA had chosen to fly Rosetta and the team felt that a comet rendezvous mission would not be selected. This consideration may not have been correct in retrospect, but the team decided to go forward only with a main belt asteroid rendezvous mission, this time to Vesta and Lutetia. In the middle of the proposal selection process, the DS1, technology validation mission was launched and some difficulty was experienced in getting the ion engines to ignite once the mission was in space. NASA apparently preferred to see the results of DS1 before selecting a Discovery mission with an ion engine. Instead they selected the MESSENGER mission to orbit Mercury and Deep Impact to explore the interior of a cometary nucleus by creating a large crater and imaging the material excavated.

The next opportunity to propose came in 2000. This time the asteroids were aligned so that a rendezvous mission to both Vesta and Ceres was possible and we decided to attempt such a mission, renaming it Dawn in reference to our attempt to understand the state of the solar system at its earliest epoch. This time DS1 had been successful in space-qualifying the ion engines that we wished to use, and the ability to orbit both Vesta and Ceres was well received by the reviewers. In January 2001 we were informed that we had been selected to compete in round 2, also known as Phase A, during which a Concept Study Report would be prepared and a site visit conducted. Three missions were selected for Phase A study. We expected only one to be ultimately selected for development.

The year 2001 was a difficult year for the Discovery program. There was not sufficient funding to begin the Phase A studies until the Spring quarter and there were no funds to begin Phase B after selection until a year later than planned. Hence the three missions under study had to slip their launch dates. Dawn's launch date had been in mid-2005; it was slipped to mid-2006 and put on a heavier, more powerful and more costly launch vehicle. The Concept Study Report was written and submitted and the site visit was scheduled for early September, 9/12/01.

On 9/11/01 when the Dawn team had gathered for a dry run of the site visit, the infamous terrorist attack on the US was launched. It became clear that no site visit would be held on the following day. We stopped our preparations and sent everyone home. Many could not get home, those overseas and those who did not want to drive across the country. However, thirteen west coast Dawn team members convoyed day and night in four cars and made it home in slightly over 48 hours, much to the relief of many children and spouses. At that point the site visit material was frozen and a copy of the materials put in a NASA vault until the site visit could be reconvened in November. The Associate Administrator was briefed in December, and before Christmas 2001 Dawn was selected. To the pleasant surprise of many so was the Kepler mission, but neither could be started because of the funding situation.

Delays in the space program are always costly and in a cost-capped program they can be lethal. While Dawn waited for funding to arrive, overhead rates went up, commitments to provide hardware weakened, administrators were rotated in and out of positions, and the orbital locations of the asteroids continued to evolve. When money began to flow in the Dawn program in January 2003, much replanning and much recosting had to be done. As this was happening another shoe dropped on Dawn. NASA had decided that projects had to carry significantly larger reserves. No extra funding was provided to cover this mandate. The money had to be obtained by descoping the project. Some reserves accrued when a laser altimeter funding plan could not be achieved within Dawn's payload allocation and the instrument was dropped from the manifest. Additionally a descoped plan was developed in which arrival at Ceres was delayed to an extended mission, that appeared to be acceptable to NASA. A Preliminary Design Review was held in November 2003, which the project felt was successful but when the project went back to NASA headquarters for the subsequent confirmation review, Dawn was denied confirmation because Ceres was no longer included in the primary mission. Various groups appealed, including the flight system contractor, Orbital Sciences Corporation who offered to forego their fee. After the successful MER (Mars Exploration Rover) landings in January 2004 Dawn was given a second hearing, a key provision of which was that Ceres could not be left to an extended mission, rather it had to be included in the primary mission. The orbital phases at Vesta and Ceres were cut to the minimum needed to achieve the full level 1 objectives and the mission was again presented to Headquarters for confirmation. This time the mission was conditionally confirmed for implementation but one of the conditions, without explanation,

was to drop the magnetometer. The project proceeded, and easily met the several conditions laid down. With the project in good health, restoration of the magnetometer was again requested and denied. The project successfully passed its critical design review in June 2004, and the spacecraft and instruments are at this writing well into fabrication.

3 Vesta

Observations from 1 AU with Hubble Space Telescope and with adaptive optics on ground-based telescopes have provided a good first order estimate of Vesta's physical properties. Our best estimate of the shape of Vesta is that it has a triaxial ellipsoidal shape with radii of 289, 280, and 229 ± 5 km with a large crater over the southern pole (Thomas et al. 1997a). Vesta has a mass of $1.36 \pm 0.05 \times 10^{-10}$ solar masses or $(2.71 \pm 0.10) \times 10^{20}$ kg (Michalak 2000). The corresponding bulk density is 3750 ± 400 kg/m³.

The deduction by McCord et al. (1970) that Vesta is a dry differentiated body covered with a pyroxene-bearing basalt whose composition was like that of the HED meteorites has been supported by many remote sensing studies e.g., McFadden et al. 1977; Feierberg and Drake 1980; Feierberg et al. 1980; Gaffey 1997). The composition of the surface is far from uniform (Binzel et al. 1997; Drummond et al. 1998). These variations are believed to reflect impact excavations and lava flows in different regions. They have not been obscured by space weathering. The southern crater also exhibits inhomogeneous composition. This inhomogeneity is believed to result from the exposure of the layering of the lower crust and upper mantle (Thomas et al. 1997a). The HED meteorites suggest that the parent body formed 4.56 Ga ago (Nyquist et al. 1997; Tera et al. 1997; Lugmair and Shukolyukov 1998). This early rapid evolution requires an early heat source probably ²⁶Al (Srinivasan et al. 1999). As mentioned above the HEDs also provide evidence for core formation up to a size of about 25% by mass, possibly as fractionally large as the terrestrial core. This core is believed to have formed within 3 Ma of the solar system's formation (Yin et al. 2002; Kleine et al. 2002). A thermal model consistent with these constraints suggests that the interior of Vesta remained hot for considerably longer than the ages of the HED meteorites derived from the crust (Ghosh and McSween 1998).

Clearly, the synthesis of the ground-based and Hubble-based imagery with the analysis of the HED meteorites has prepared us well for the Dawn mission. We have a useful measurement of the mass enabling us to calculate the required fuel load to execute the orbital maneuvers needed. We know the rough shape and surface area of Vesta so we can plan our observational program. We know the albedo so we can plan exposures for the camera. We know the color variation and spectral features to enable us to choose the correct filters to install in the camera.

Nevertheless, there are some areas where improvements can be made in our measurements. The initial set of Hubble images were made in 1994 with the Wide Field Planetary Camera (WFPC 2) with 52 km/pixel resolution (Thomas et al. 1997b). In 1996 with Vesta much closer to Earth, WFPC 2 was used to obtain images with 36 km/pixel resolution (Thomas et al. 1997a) but these data have not yet been fully analyzed. More recently a new improved imager has become available, the High Resolution Channel in the Advanced Camera for Surveys. This camera has been used for Ceres but has not yet been used to obtain improved imagery of Vesta.

One area of improvement needed for Dawn is knowledge of the orientation of Vesta's pole. From their 1994 observations Thomas et al. (1997a) place it at right ascension $308^\circ \pm 10^\circ$ and declination $48^\circ \pm 10^\circ$ but they did not update this value with their later

1996 observations (Thomas et al. 1997a). In contrast Drummond et al. (1998) find a pole of right ascension $333^\circ \pm 2^\circ$ and declination $43^\circ \pm 2^\circ$. These two observations disagree by an amount inconsistent with their stated error bars. Even if there were not a contradictory measurement, the size of the error bars based on the HST observations are too large to be used in mission planning such as to determine the illumination of the poles upon arrival and departure at Vesta. It would be very helpful to obtain a second set of accurate data to validate the Drummond et al. (1998) measurements. Moreover, Drummond et al. (1998) suggest that Vesta is not rotating about its principal axes of inertia. This too should be verified. More AO and HST observations of Vesta are clearly needed.

Because the global surface composition of Vesta is very similar to that of the HED meteorites, continued study of the HEDs is also important even though Vesta itself may not be the immediate source of these meteorites. The traditional scenario is the following: great impacts excavated the surface of Vesta and produced a swarm of small fragments. Some of them approach the chaotic region associated with the 3:1 resonance from where fragments can be rapidly transferred to Earth crossing orbits. Further collisions ejected fragments into Earth-colliding orbits, becoming the HED meteorites recovered on Earth. This hypothesis was confirmed by the identification of a Vesta dynamical family (Williams 1989; Zappalá et al. 1990) and the discovery that these objects have a surface composition similar to Vesta (Binzel et al. 1993; Burbine et al. 2001).

In recent taxonomies, asteroids showing a spectrum similar to that of Vesta have been classified as V-type (Tholen and Barucci 1989), while the name “Vestoids” was initially used by Binzel et al. (1993) to refer to all the asteroids in the region near Vesta having a V-type spectrum. The spectroscopic link between the Vestoids, the V-type asteroids in the vicinity of Vesta and in near-Earth orbits, and the HED meteorites seems to be quite consistent, especially if we take into account that basaltic material is very rare in the asteroid belt. However, some problems still remain open. For example, the cosmic ray exposure time observed in the HED meteorites seems to be incompatible with the transport dynamical time of the NEAs (Migliorini et al. 1997). The spectra of all the HED meteorites show a subtle absorption feature, which is observed only on some V-type asteroids in the Vesta region (Vilas et al. 2000). Moreover, the V-type asteroids in the Vesta region present a spectra with a 1-micron band, deeper than most of the Vestoids and Vesta itself. This suggests the possible coexistence of two distinct mineralogical groups, either probing different layers of Vesta or coming from different bodies; hypothesis already raised by (Vilas et al. 2000). On the other hand, if all the V-type asteroids actually come from Vesta, then the apparently different groups might be explained by two large impacts on Vesta excavating layers of different materials (Marzari et al. 1996) or a single energetic impact, which ejected fragments from the inner layers of Vesta’s crust. It is worth recalling that the crust of the HEDs’ parent body is associated with two different mineralogies: (i) a diogenite lower crust and (ii) an eucrite upper crust. Hydrocode models simulating the fragmentation of Vesta (Asphaug 1997) indicate that the material from both the crust and the mantle may actually be ejected. A recent study (Kelly et al. 2003) confirmed that at least one Vestoid, 1929 Kollaa, has compositional characteristics compatible with cumulate eucrite, which suggests that it has been formed deep inside the eucritic crust of Vesta.

As noted above the HED meteorites indicate that Vesta formed a metallic core. The loss of the magnetometer from the mission lessens Dawn’s ability to probe the core. Estimates of its mass from cosmochemical analysis range from 0 to 25%. If the range of this number could be narrowed, we could increase our understanding of Vesta’s interior. Reports like that of a quartz veinlet in HED meteorites (Treiman et al. 2004) as illustrated in Fig. 4 also bring knowledge of the possible history of Vesta that is unattainable from space. Remote

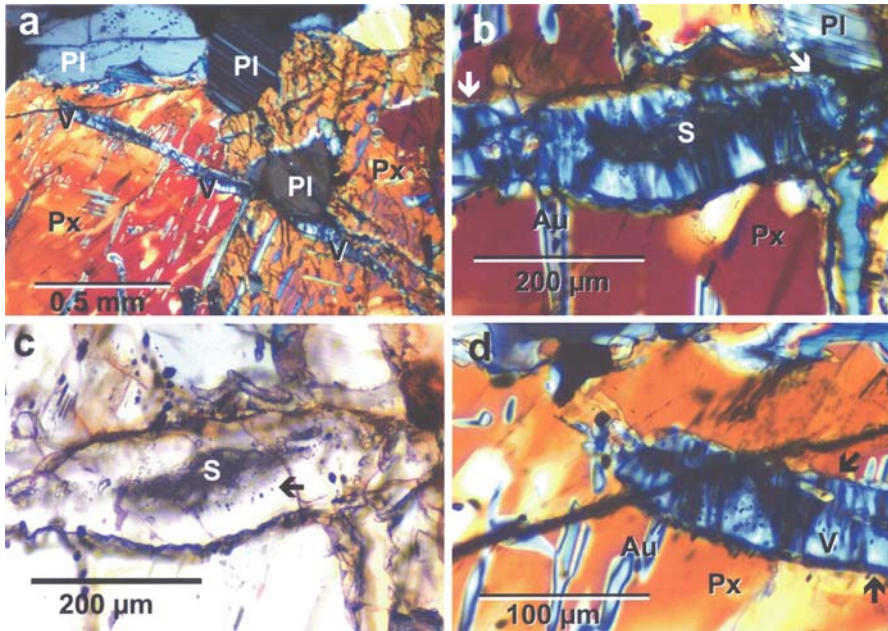


Fig. 4 Quartz veinlet in Eucrite suggesting water existed for at least a short time on the surface of Vesta (Treiman et al. 2004). Thickest portion of veinlet shown between arrows in panel b. See TBD for color version

sensing measurements (e.g., Hasegawa et al. 2003) also have been interpreted as indicating the alteration of surface materials by water. In short, we need to continue the interaction of the ground and space communities through the period of the rendezvous and subsequent analysis of the data.

4 Ceres

In the absence of information about a specific object we tend to hold ideas based on stereotypes. Thus there is a tendency to consider Ceres as resembling a big carbonaceous chondrite because we have very, very little information about the physical state and chemical composition of Ceres. In particular we have no meteoritic evidence bearing on Ceres and its thermal evolution. We do in fact know that the surface of Ceres is not carbonaceous (Gaffey and McCord 1978). In particular it contains spectral features of an aqueous alteration product. That no meteorites could be firmly correlated to Ceres may be an important clue about the composition of the crust of Ceres. Our inability to find Ceres meteorites could be explained by Ceres' crust consisting of a material that is common in the solar system, which could survive on Ceres for eons but would not survive the trip from Ceres to Earth. Water-ice is such a material.

In contrast the size and shape of Ceres are now well understood. McCord and Sotin (2005) have reviewed the mass and shape determinations in the literature and have concluded that the mass of Ceres is $4.74 \pm 0.026 \times 10^{-10}$ solar masses or $(9.43 \pm 0.05) \times 10^{20}$ kg. More recently Thomas et al. (2005) have shown using 2003/2004 observations from the High Resolution Channel of the Advanced Camera for Surveys that

Ceres is an oblate spheroid with an equatorial radius of 487 ± 2 km and a polar radius of 455 ± 2 km and a rotational pole with a right ascension of 291° and a declination of 59° . The shape is similar to that of a Maclaurin spheroid. For a body in a relaxed state whose density is Ceres' observed 2100 kg/m^3 and whose period is 5.34 hours, the observed flattening is consistent with a central condensation or core (Thomas et al. 2005). A core of rock with a mantle of water ice can explain this central condensation and Ceres' average density. For a body and a mantle of water ice we would expect such relaxation (Slyuta and Voropaev 1997). Ceres physical properties are thus consistent with its having a thick outer mantle of water ice and possibly even a global ocean of water beneath that ice. This hypothesis has received substantial support in a recent model of Ceres' thermal evolution (McCord and Sotin 2005). Their model shows that Ceres can plausibly retain its primordial water and possibly even a global ocean over the period since accretion.

If Ceres has a crust and a mantle of water ice, we can understand why there is no meteoritic evidence for the composition of Ceres but why have we not seen evidence for ice on Ceres in the past? That Ceres could retain its water beneath a rocky surface was supported theoretically long ago (Fanale and Salvail 1989). However, the existing paradigm has been one in which Ceres was thought to be more like Mars than like Callisto, the iciest Galilean satellite. However, there are similarities of Ceres to Callisto. Calvin and Clark (1993) point out that the absorption feature near 3.1 microns on Callisto is similar to that in the spectrum of Ceres, where it was attributed to NH_4 -bearing clays (King et al. 1992). If there is a hard ice crust on Ceres as produced in the model of McCord and Sotin (2005), then clays formed from the inevitable dust mantle caused by meteorite impacts on Ceres are not hard to imagine.

There is additional evidence for water on Ceres. A'Hearn and Feldman (1992) have reported OH above the sunlit pole after perihelion as if a polar cap of water ice were subliming. A similar explanation was given for a change in the reflectance spectrum of Ceres when its north pole received maximum sunlight (Golubeva and Shastopalov 1995). If these observations are not artifacts, then they indicate that water vapor is escaping through the crust and any dust mantle above it.

Images of the surface of Ceres as well as measurements of its shape also seem to be consistent with the icy planet scenario. No obvious surface relief is seen on the images, no mountain ranges on the limbs. The surface brightness is fairly uniform varying by about 0.1 magnitude with one very notable exception. Figure 5 shows three images that illustrate the rotation of a UV bright spot on the Ceres surface that was used by Thomas et al. (2005) as their control point for mapping. A similar bright point is seen in the adaptive optics photos by C. Dumas (personal communication, 2002) one of which is shown in Fig. 3. There is only one such bright point in the HST images. The simplest explanation is that it is due to an impact crater that has excavated to a layer below the dust mantle. If it is water ice

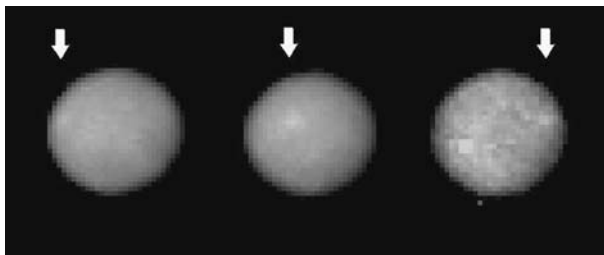


Fig. 5 Three images of Ceres illustrating the rotation of a bright spot on the surface (Thomas et al. 2005)

we would expect such a structure to sublime with time (Fraser and Salvail, 1989) and to again become covered with dust.

As with Vesta it is clear that an orbital mission is necessary to resolve these questions, but Dawn does not arrive at Ceres until 2015. There is much that can be done from 1 AU before then. We should first try to determine what is the nature of the bright albedo feature on Ceres. Data were obtained on Ceres' albedo at three wavelengths 220 nm, 330 nm and 555 nm in 2003/2004. These do reveal interesting brightness and albedo variations (Li et al. 2006). Second, can the inferred sublimation events be confirmed? We know the rotation pole of Ceres well enough to predict when the effect will be seen. Clearly, there are many opportunities for the space and 1 AU communities to work together in understanding Ceres.

5 Instruments

Dawn carries three scientific instruments: a pair of framing cameras; a visible and infrared mapping spectrometer, and a gamma ray and neutron detector. Dawn also measures the gravitational field with the use of its radiometric tracking system. Images are used for navigation and also for topography in addition to characterizing the properties of the surface. In this section we describe the properties of the three instruments and the gravity investigation.

5.1 Framing Camera

Two identical framing cameras have been designed and are being built by MPS in Lindau Germany in cooperation with DLR Berlin and IDA Braunschweig. These will provide images of the surface of Vesta and Ceres and will also be used for navigation. The camera (shown in Fig. 6) uses an f:1/8 rad-hard refractive optics with a focal length of 150 mm. The field of view of $5.5^\circ \times 5.5^\circ$ is imaged onto a frame-transfer CCD with 1024×1024 sensitive pixels. With a pixel pitch of 14 μm the camera samples the scene at 9.3 m/pixel from a distance of 100 km. Two identical camera systems including data processing units will be delivered to provide redundancy critical for optical navigation operations. One camera head consists of the housing, refractive lens system, filter-wheel, focal plane, and readout electronics with 2.5 kg total mass and 1.8 W power consumption. The data processing unit controls the camera and handles the data by compressing and buffering them. Data compression of the 14-bit samples is implemented by software based on wavelet algorithms. Compression rates can be selected from lossless (about 2:1) to lossy 10:1 (and more) which still provides acceptable images.

The filter wheel has eight positions and is equipped with one clear filter and seven multispectral filters. The clear filter is used to support spacecraft navigation and for high signal-to-noise (SNR) observations, e.g., imaging at exposure times much less than the dwell time to enhance image contrast and sharpness of morphologic features, to search for dust at forward scattering observation geometries, as well as high-speed imaging at low altitudes. Except for the clear filter covering the range 450–950 nm and the 980 nm filter with a full-width-half maximum (FWHM) of 80 nm, all spectral channels have 40 nm FWHM. The sensitivity is sufficient for the surfaces of Vesta and Ceres to be imaged in each filter with a SNR of 100 for exposures from 100 ms to 1 s. At lowest altitudes when blur might occur in longer duration color exposures the clear filter and shorter (25 ms)

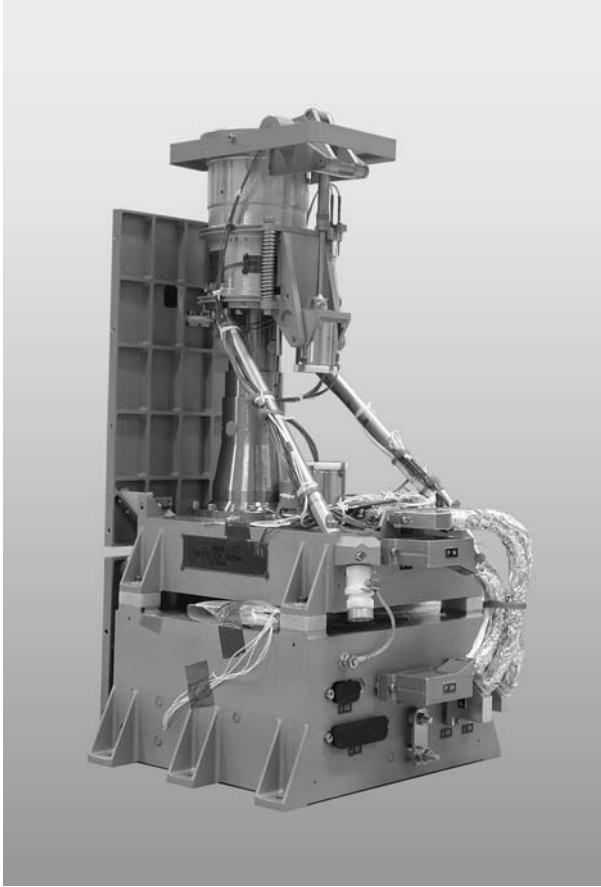


Fig. 6 The Dawn framing camera

exposures are used. A stray light baffle shades the pupil from reflections from the spacecraft body and allows imaging as close as 20° sun avoidance angle.

The camera operates at a readout rate of 1 Mpixel/s or 1 s per 1024×1024 frame. The minimum exposure time is 1 ms. To improve the SNR of the data, pixels can be binned under software control or subarrays selected to increase the read out frame rate. The digital processing unit has 16 Gbit of gracefully degrading instrument related memory equivalent to 1000 uncompressed pictures. Each Data Processing Unit (DPU) consumes between 2 and 5 W and weighs 2.5 kg. The total resources per camera are 5 kg of mass and circa 12 W consumption. A reclosable cover is used in front of the optics to protect against contamination from external sources. Dedicated heaters on the focal plane detectors are used to drive off possible condensing contaminants, to provide for annealing of the detector to reduce radiation damage, and to maintain favorable temperature gradients during long cruising intervals. The command software is high level and based on the operating system developed for OSIRIS (Science imagers for the Rosetta mission) and VMC (Venus Monitoring Camera).

The design of the camera is based on several lines of heritage. The DPU is essentially a copy of the unit for VMC on Venus Express. In particular the software is the same as

developed for OSIRIS and VMC with very minor adaptations for Dawn. The optical design is conservative and promises excellent performance based on the detailed phase A study. The detector and read out electronics are copies of the units implemented in the ROLIS Down-looking Imager on the Rosetta lander. There are two mechanisms: a filter wheel operated by a Geneva-type drive and an optics cover. The lightweight filter wheel itself is based on a design flown in the Halley Multicolour Camera of the Giotto mission. A similar drive concept (but reciprocating) was built by MPS for the protective cover drive of the optics in the Robotic Arm Cameras of the Mars Polar Lander and the 2001 Mars Surveyor Lander. The optics cover incorporates a fail safe release mechanism. Both mechanisms are driven by identical stepper motors; motors of the same type (but larger) were successfully flown on missions like SOHO.

5.2 Visible and Infrared Mapping Spectrometer

The Dawn mapping spectrometer (VIR) shown in Fig. 7 is a modification of the VIRTIS mapping spectrometer (Coradini et al. 1998; Reininger et al. 1996) on board the ESA Rosetta mission. It will be operated to map the compositions of Vesta and Ceres for 2 years and spend 10 years in space. It derives much design heritage from the Cassini VIMS spectrometer with an operational lifetime of > 4 years and a mission life > 10 years. The

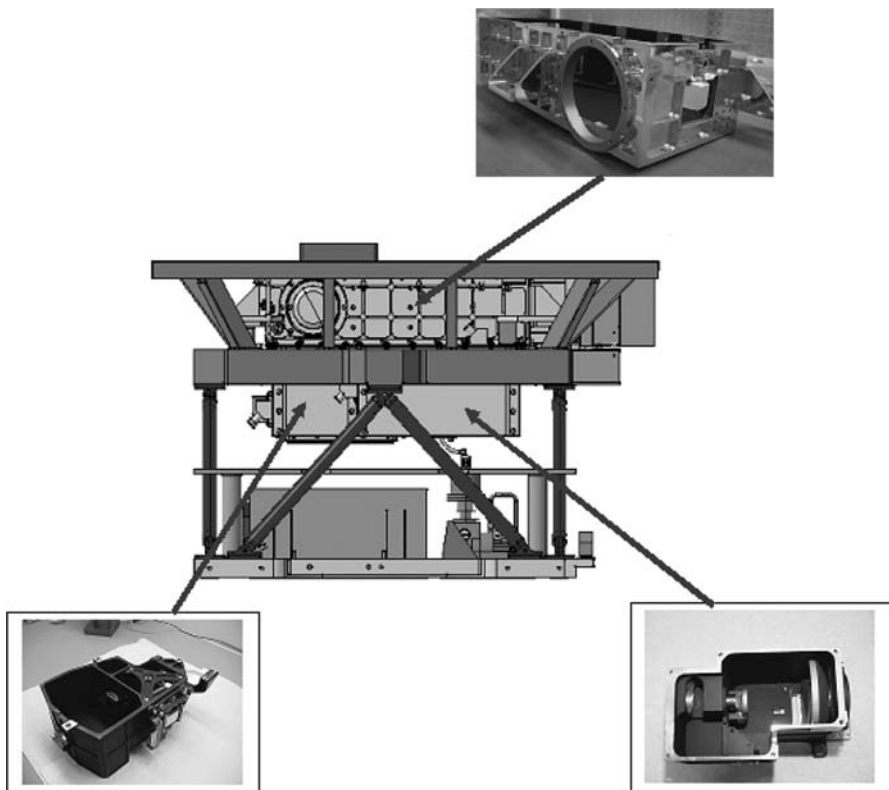


Fig. 7 The VIR mapping spectrometer with some of its subassemblies: top, scan mirror and baffle assembly; bottom right, telescope subassembly; bottom left, spectrometer subassembly

design fully accomplishes Dawn's scientific and measurement objectives. VIR is an imaging spectrometer that combines two data channels in one compact instrument. The visible channel covers 0.25–1.0 μm while the infrared channel uses a mercury cadmium telluride infrared focal plane array (IRFPA) to image from 1 to 5 μm . The use of a single optical chain and the overlap in wavelength between the visible and the infrared channels facilitates inter-calibration. The VIR instantaneous field of view is 250 m/pixel at a distance of 100 km while the full field of view is 64 mrad.

The spectrometer consists of three modules: optical system (5.0 kg mass); proximity electronics (3.0 kg and 5 W); and cryocooler including driving electronics (1.3 kg and 12.6 W). A mechanical and thermal mounting structure of 5.0 kg mass accommodates the spectrometer subsystems. The optical system, which includes foreoptics, dispersive elements, filters, focal plane assemblies as well as the cryocooler and proximity electronics is a complete re-build of the Rosetta VIRTIS mapping spectrometer.

The optical concept is inherited from the visible channel of the Cassini Visible Infrared Mapping Spectrometer (VIMS-V) developed at Officine Galileo and launched on Cassini in October 1997. This concept matches a Shafer telescope to an Offner grating spectrometer to disperse a line image across two FPAs. The Shafer telescope is the combination of an inverted Burch off-axis telescope with an Offner relay. By putting an aperture stop near the center of curvature of the primary mirror, coma is virtually eliminated. The result is a telescope system that relies on spherical mirrors, yet remains diffraction limited over a large spectral range and the whole spatial direction. The horizontal field is realized by rotating the telescope primary mirror around an axis parallel to the slit. The Offner spectrometer is matched to the telescope, and does not rely on a collimator and camera objective. This is possible because both telescope and spectrometer are telecentric and the telescope has its exit pupil on the grating.

The spectrometer does not use beam-splitters. Two different groove densities are ruled on a single grating. The central regions of the grating, which make up the central 30% of the conjugate pupil area, correspond to the higher groove density needed to generate the higher spectral resolution required in the visible channel extending from the ultra-violet to the near infrared. The infrared channel utilizes the outer 70% of the grating, which is ruled with a lower groove density. The larger collecting area in the infrared compensates for the lower solar irradiance in this region. The grating profiles are holographically recorded into a photoresist and then etched with an ion beam. Using various masks the grating surface can be separated into different zones with different groove densities and different groove depths.

The visible detector array is based on the Thomson-CSF type TH 7896 CCD detector. It uses a buried channel design and poly-silicon N-MOS technology to achieve good electro-optical performance. Moreover it includes a multi-pinned phase (MPP) boron implant to operate fully inverted in order to substantially decrease the surface dark current, residual images after strong exposure, and other effects due to ionizing radiation. The TH7896M is a full frame image sensor with 1024×1024 sensitive elements, two registers and four outputs. It is used as a frame transfer device with a sensitive area and a storage area. The first half is used to acquire the data and the second half is used to send the data to the proximity electronics to be converted.

The IR detector used in the spectrometer is based on a bidimensional array of IR-sensitive photovoltaic mercury cadmium telluride coupled to a silicon CMOS multiplexer. The device is an array of 270×435 HgCdTe photodiodes manufactured by Raytheon Infrared Center of Excellence (Santa Barbara USA) with a spacing of 38 μm between diode centers. The spectral wavelength range is 0.95 to 5.0 μm and an operating temperature of 70 K. The detector is packaged into a housing which includes an optical

window which provides suitable mechanical, thermal and electrical interfaces for its integration on the focal plane. Furthermore, the window functions as substrate for the order-sorting filters. These filters are used to stop the superimposition of higher diffraction orders coming from the grating and also to reduce the background thermal radiation from the instrument housing. The transmission characteristics of the window are optimized for each corresponding detector position, so that for each filter zone only the designed wavelength range corresponding to the first diffraction order is allowed to pass. Six segment filters are coated in the window with the following bandpasses: 0.9–1.6, 1.2–1.9, 1.9–2.5, 2.4–3.75, 3.6–4.4, 4.3–5.0 μm .

In order to minimize the thermal background radiation seen by the IR-FPA, the spectrometer itself needs to be cooled to less than 135 K by radiating at least one, or possibly two of its surfaces toward cold space. Such a configuration also provides the operational temperature needed for the CCD. The IR-FPA requires an operating temperature of 70 K to minimize detector dark current, which is achieved by using a Stirling active cooler driven by dedicated electronics. The Stirling cooler that best meets VIR's requirements is the RICOR K508 tactical cooler. It is an integral cooler in which the regenerator, where the heat exchanges at warm and at cold temperatures occur, is directly connected to the compressor. Without the transfer line characterizing the split cooler, less heat losses occur and more efficiency is reached. On the other side, due to the internal balancing device and the reduced heat flow from the compressor to the cold finger, vibration and heat transmitted to the regenerator and to the cold end (where the FPA is connected) are very limited.

A cover in front of the optics entrance aperture protects against contamination from external sources. Dedicated heaters on the focal plane remove possible condensing contaminants and provide for annealing of the detector to reduce radiation damage. The cover-inside is coated and used as calibration target in combination with two internal calibration lamps (one for the VIS-FPA and one for the IR-FPA).

5.3 Gamma Ray/Neutron Spectrometer

The Dawn gamma-ray and neutron detector (GRaND) shown in Fig. 8 maps the abundance of rock-forming elements (O, Si, Fe, Ti, Mg, Al, and Ca), radioactive elements (K, U, and Th), trace elements (Gd and Sm), elements such as H, C, and N, which are the major constituents of ices. It draws on decades of experience at LANL in measuring neutrons and energetic photons and is an improved version of the highly successful Gamma Ray Spectrometer (GRS) on Lunar Prospector (LP), and the presently operating Neutron Spectrometer aboard Mars Odyssey (MO). The design of the spectrometer and its expected performance is described in detail by Prettyman et al. (2003). The gamma-ray sensor is segmented into two parts and the neutron sensor into four parts. Onboard classification of the multiple signals from each event then allows directionality determination that can discriminate radiation of asteroid and spacecraft origin. The gamma-ray sensor is a squared-off version of the LP bismuth germanate (BGO) scintillator. In addition, a 4×4 array of 0.75 cm^3 cadmium zinc telluride (CZT) sensors are located on the side facing upward from the deck toward the asteroid. The CZT sensors are a new technology demonstration (Prettyman et al. 2002). The gamma ray sensors are surrounded by four segments of an anticoincidence shield (ACS) made using a borated plastic scintillating material. Each of the four segments is viewed by a separate phototube. The upward (asteroid) and downward (spacecraft) facing boron-loaded plastic segments are optically coupled to a ^6Li loaded glass scintillator. The sides of the upward and downward facing

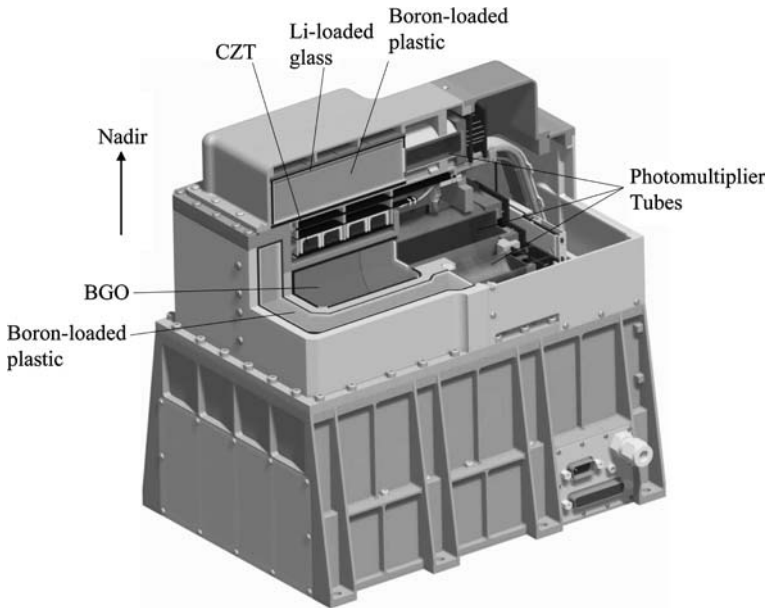


Fig. 8 The GRaND gamma ray and neutron detector

segments are wrapped in Gd foil. The combination of the Gd and ${}^6\text{Li}$ glass shield the borated plastic from thermal neutrons. Consequently, the borated plastic scintillator is sensitive only to epithermal and fast neutrons, which are separated electronically as was done for the Lunar Prospector and Mars Odyssey instruments. The ${}^6\text{Li}$ glass absorbs thermal and epithermal neutrons. The epithermal contribution can be removed to determine the thermal neutron count rate by subtracting a portion of the epithermal count rate from the plastic from the total count rate from the glass.

The Dawn GRaND data at Vesta and Ceres will be of comparable quality to that of the LP neutron spectrometers. The CdZnTe sensor has a factor of four higher spectral resolution than that of the LP gamma-ray spectrometer, enabling unprecedented accuracy for elemental analysis: The CZT fully resolves gamma rays from most elements of interest. Simulations verify that our present design provides a robust neutron and gamma-ray signal strength at Vesta and Ceres, adequately controls spacecraft backgrounds, yields a robust BGO spectrum that is as good or better than that measured using the LP GRS BGO detector and is effective in suppressing the background from the spacecraft. If the CZT detector fails to achieve optimal resolution e.g., because of radiation damage in the space environment, the Dawn GRaND science objectives are still met. We have shown that annealing of CZT at moderate temperatures (40–60°C) for short periods of time can fully restore resolution following radiation damage. The exposure predicted for the CZT behind the ACS is low enough that we do not anticipate significant degradation in performance due to radiation damage. However, to ensure performance, our design includes the capability to anneal the CZT array if damage is observed (Prettyman et al. 2003).

The Dawn GRaND consists of a 7.6 cm wide \times 7.6 cm long \times 5 cm high rectangular slab of BGO that is viewed by a 5 cm diameter photomultiplier tube (PMT). A 4×4 square array of 0.75 cm^3 CZT sensor element is positioned above the upward BGO face (away from the spacecraft deck facing the asteroid). The BGO acts as an active shield,

minimizing spacecraft contribution to the response of the CZT array. This compound gamma-ray sensor is surrounded on five sides by a rectangular borated plastic ACS that is composed of four separate elements, each viewed by its own 2.5 cm diameter PMT. The thickness of the up and down plastic scintillator elements is 2.5 cm and that of the two L-shaped side elements is 1 cm. The top and bottom ACS elements are laminated by 2 mm thick ^6Li glass scintillator sheets, which are viewed by the same PMTs that view the plastic to which they are optically coupled. The top and bottom ACS faces are surrounded on their sides by 0.046 cm thick sheets of Gd to prevent access by thermal neutrons from the spacecraft.

The front-end electronics for the BGO and ACS portions of the GR/NS are configured to classify each detected event into one of five categories. These categories are identical to that used on LP and MO. The five categories are: (1) an isolated BGO interaction, (2) a single coincident BGO and ACS interaction, (3) a subset of these coincident interactions where the energy deposited in the BGO and ACS are defined by window discriminators to fall within narrow ranges centered on 478 keV in the BGO and 93 keV in the ACS, (4) a single ACS interaction, and (5) a time-correlated pair of ACS interactions that occur within 25.6 μs . Addition of the CZT sensors adds four additional categories: (1) an isolated CZT event, (2) a coincident CZT and BGO interaction, (3) a subset of these coincident events where the energy deposited in the BGO is 0.511 ± 0.075 MeV, and (4) a coincident CZT and ACS interaction where the energy deposited in the CZT and ACS are defined by window discriminators to fall within narrow ranges centered on 478 keV in the CZT and 93 keV in the ACS. Simulated spectra have demonstrated the capabilities of these hybrid CZT-BGO detector operation modes.

All information is packaged in a 3.1 kb/s data string with an accumulation time of 60 s. A 478 keV gamma ray from $^7\text{Li}^*$, which is produced by neutron capture by ^{10}B , provides a continuous calibration of gain as proven on LP. Gamma-ray spectra, both accepted and rejected by the ACS are recorded separately and telemetered to Earth. Thermal neutrons from the asteroid are measured using the ^6Li loaded glass of the upward-facing ACS element and those from the spacecraft use the ^6Li loaded glass of the downward-facing element. Separation of the Li-glass from the boron loaded plastic will be implemented using pulse amplitude discrimination.

Epithermal neutrons having energy in the range between about 0.2 eV and 0.5 MeV from the asteroid are measured using the upward ACS element in coincidence with a 478 keV CZT or BGO interaction. Those from the spacecraft use the downward ACS element in coincidence with a 478 keV BGO interaction. Fast neutrons having energies between about 0.5 MeV and 8 MeV are measured using the ACS by isolating double interaction events. The pulse height of the first pulse of the pair provides a measure of the energy of the incident fast neutron.

Overall, GRaND is a relatively simple instrument that delivers significant science. The gamma ray and neutron sensors were selected and configured to suppress and separately measure the spacecraft background, providing accurate measurements of neutron and gamma ray leakage spectra from each asteroid. There are three basic modes of operation and no moving parts. The telemetry rate is relatively low, 3.1 kbps. The mass of the instrument is approximately 10 kg and the power consumption is 9W.

6 Gravity Science and Shape Modeling

The objectives of the gravity investigation are to determine the masses of the asteroids, their principal axes, rotational axes, and their moments of inertia, as well as derive models

of the global gravity field of Vesta to the 10th harmonic degree and order, and of Ceres to the 5th harmonic degree and order. The objectives of the shape investigation are to develop near-global (>80% of surface) maps of the shapes of Vesta and Ceres to contribute to knowledge of the surface evolution and internal structure of these asteroids. Mass together with the shape model determines the bulk density. The shape and gravity models can be combined to characterize crustal and mantle density variations (e.g., Zuber et al. 2000), and together with any detectable wobble in rotation, can provide information on the possible differentiation and formation of a core. Present estimates of the fractional radius of the (presumed metallic) core of Vesta range up to 50%, corresponding to a fractional mass of up to 20%. If Ceres accreted water ice during formation as it presently appears, we do not expect it to be differentiated. The principal axes are determined directly from the second-degree harmonics of the gravity field. The polar moment of inertia (homogeneity constant) constrains the radial density distribution. Presently the densities of Ceres and Vesta are known to 2% and 3% respectively from perturbations on other asteroids and their optically determined shapes (Hilton 1999; Konopliv et al. 2002). The Dawn science objective is to measure the bulk density to better than 1% and Dawn will achieve relative accuracies near 0.1%.

The gravity field is determined in loose, medium and tight orbit states. In the initial “loose” orbit, only the mass is determined while optical images determine the rotational state. In the optical mapping (medium) orbit, the gravity field is determined to about degree 4. In the low altitude mapping orbit, an altitude which is below one body radius at Vesta, the gravity field is determined up to the 10th degree. With a 10th degree gravity field, correlations with surface features on Vesta of 90 km or greater block size can be investigated, including the large 460 km impact basin near the south pole (Thomas et al. 1997a). This higher resolution gravity field allows for comparative modeling with lunar impact basins (Zuber et al. 1994). During gravity tracking passes, Dawn uses reaction wheels for attitude control, thus minimizing disturbances due to thruster firings, and improving the accuracy of the gravity field determination. The altitude of the lowest mapping orbit on Ceres will resolve variations of scale 300 km or greater, unless the orbit can be lowered.

The shapes of Vesta and Ceres will be determined using images from the framing camera in concert with radiometric tracking. A control point network will be derived and used to develop a geodetic grid in a planetary center of mass coordinate system. This geodetic grid will be used to obtain the basic shape parameters. Stereo images and photoclinometry will be utilized to fill in gaps between control points for studies of higher resolution morphology. The resolution of the shape model for Vesta will be ~100 m spatial and 10 m vertical, and for Ceres ~200 m spatial and 20 m vertical.

To use the bulk density to model the interior structure requires measurement of the polar moment of inertia (C). A 1% determination of C would significantly constrain core size and composition. The detection of a wobble off the principal axes is necessary to enable C to be determined. For the NEAR mission, the detection of a 0.1° wobble would have determined C for 433 Eros to 1% (Miller et al. 1995), but no wobble was detected that was greater than 0.01° (Konopliv et al. 2002). Similar to NEAR, Dawn will look for a possible Vesta and Ceres wobble by precise photogrammetric mapping and radiometric tracking. Any present-day wobble would indicate a recent impact or impacts.

The navigation team collaborates with the gravity science and imaging teams, and involves processing data from the Framing Camera. The image-based control point network used to develop a geodetic grid is also required for accurate navigation. Shape observations are needed for mission planning, and gravity field determination is needed for

orbit determination. The work of these teams must be closely coordinated to optimize the science return and minimize duplication of effort.

7 The Spacecraft

The Dawn spacecraft uses solar power to ionize its xenon fuel, and accelerate the xenon to velocities up to 31 km/s. The efficiency of its engines depends on the available power so when the solar illumination drops as it does at large solar distance, the decreased thrust cannot simply be recovered by firing the thrusters longer. The fuel is used less efficiently at very low thrust levels. This sets a minimum power level that the spacecraft must provide at Ceres, which can be close to 3 AU at aphelion, and which in turn governs the size of the solar arrays. Thus Dawn, shown with solar panels deployed in Fig. 9, is a large spacecraft almost 20 m from solar panel tip to solar panel tip, capable of generating 10.3 kW of power at 1 AU. The main structure of the spacecraft is about 1.4 m on a side. The axis about which the solar array rotates is the x-axis. Generally the x-axis is oriented perpendicular to the solar direction and the panels oriented around the x-axis to receive maximum illumination. While in orbit and not thrusting, the instrument deck, or z panel, shown on top of the spacecraft in Figs. 9 and 10 is pointed toward the asteroid, i.e., nadir. The three ion thrusters mounted on the opposite or $-Z$ side of the spacecraft and are gimbaled to enable them to always thrust through the center of gravity of the spacecraft. Only one ion thruster is used at a time. The High Gain Antenna used for communication with the Earth is fixed on the $-Y$ panel of the body of the spacecraft and therefore the spacecraft attitude in general must be changed and thrusting stopped during communication sessions. Similarly during the nadir pointing observation periods the thrusting is off and pointing is optimized for solar power and body viewing. Figure 10 shows a close-up of the spacecraft configuration and many of the instruments and subsystems attached to the outside of the spacecraft.

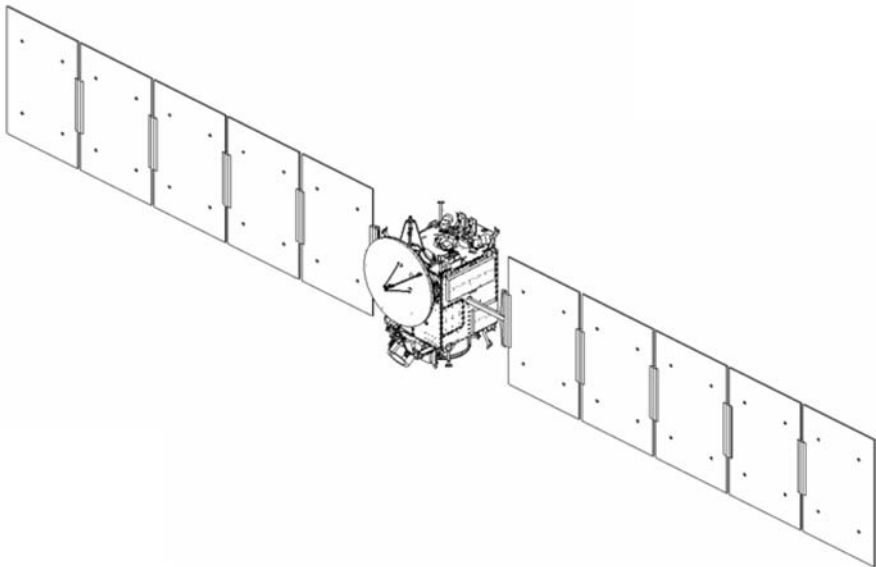


Fig. 9 The Dawn spacecraft showing the full extent of the 20 m tip to tip solar array

The spacecraft carries 450 kg of xenon fuel that is used to take the spacecraft from Earth to Vesta via Mars and then Vesta to Ceres, as well as for orbital operations. Pointing of the spacecraft can be controlled by reaction wheels and by hydrazine thrusters.

The design of the Dawn flight system includes much heritage from previous Orbital Sciences Corporation and JPL spacecraft, including low Earth orbit, geosynchronous orbit and deep-space missions. Significant redundancy in flight systems has been included so that the spacecraft is protected against many single point faults. Dawn has 8 Gb of mass memory for buffering the data before transmission. Much of the flight software is inherited from previous projects. Our present best estimate for the mass of the spacecraft with the hydrazine and excluding the xenon is 723 kg. A more detailed description of the spacecraft has been written by Rayman et al. (2006).

8 Launch and Interplanetary Trajectory

The Dawn spacecraft is scheduled for launch in June 2006 on a Delta 2925H. While a direct trajectory to Vesta is possible with the current best estimate of mass and power from

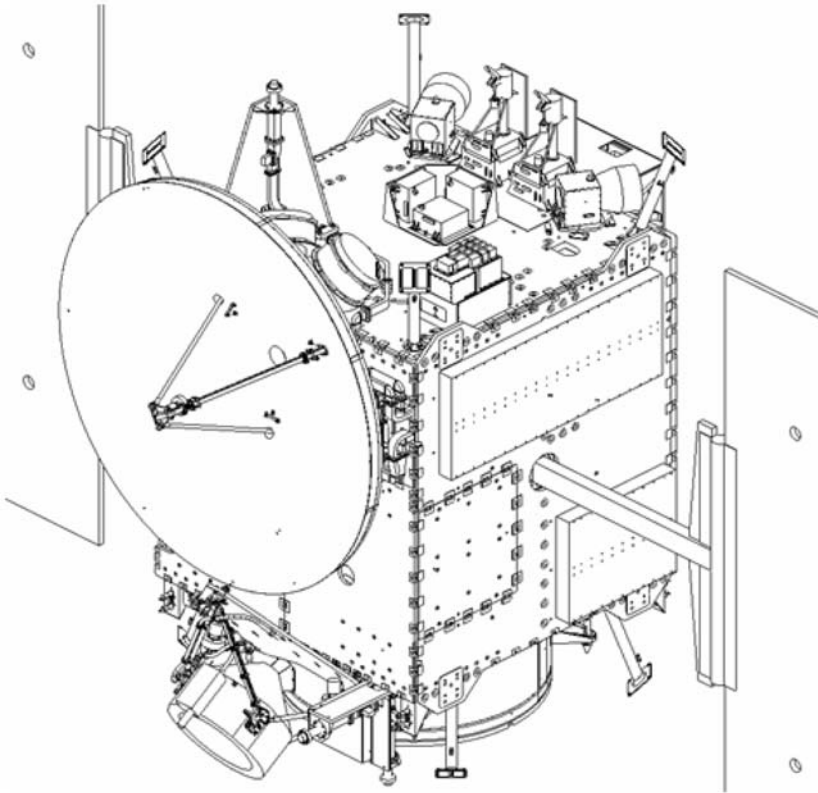


Fig. 10 The central “core” structure of the Dawn spacecraft showing the back of the high gain antenna on the right and one of the ion thrusters on the lower left. VIR is on the top of the same panel looking vertically. The two framing cameras sit directly above VIR but on the top deck-GRaND is in the far corner on the top desk

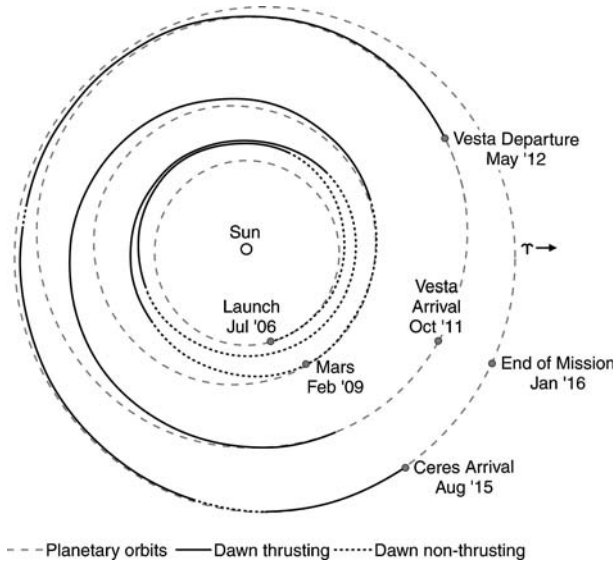


Fig. 11 Dawn’s interplanetary trajectory in heliocentric coordinates. Solid lines are drawn where Dawn is thrusting; dashed lines where the thrusters are off. The orbits of Earth (thin solid line) and Mars, Vesta and Ceres (thin dashed lines) are also shown

the solar array, a flyby of Mars provides greater technical margins at the expense of longer time to arrive at Vesta and Ceres. This trajectory is shown in Fig. 11. The portion of the trajectory that is dashed in Fig. 11 is when the spacecraft is not thrusting. It does not have to thrust immediately after launch nor in the period around the Mars gravity assist in March 2009. Once the thrusters are reignited after the Mars gravity assist, they are used almost continually to get to Vesta and almost continually from Vesta to Ceres. The spacecraft schedules a short hiatus from thrusting every week so that it can orient its antenna to Earth and send data and receive commands.

While Fig. 11 shows the spatial configuration of the trajectory well it does not provide an intuitive picture for the interplanetary time line. Figure 12 shows the mission milestones versus time with the orbital segments and the increasingly long thrust periods clearly shown. The spacecraft range to Earth controls the data rate available. Vesta orbit occurs at a particularly propitious time while Ceres orbit occurs near the greatest possible distance when the data rate is least. When the Sun-Earth-probe angle is near 180° the spacecraft is high in the night sky and far from radio interference from the Sun. However, when this angle is near zero the solar conjunction interferes with radio communication. This is not a consideration at Vesta but is a consideration at Ceres.

The nominal mission plan is to arrive at Vesta in October 2011 and leave in May 2012 to arrive at Ceres in August 2015, with an end of mission in January 2016. For planetary protection purposes the spacecraft has to be left in a safe orbit around Ceres so that it does not crash for at least 50 years. Fortunately, as we have learned more about Ceres from our HST observations it appears that Ceres provides a gravitational field that will facilitate longevity of the orbit.

A consideration in designing a planetary mission is having adequate reserves to meet any credible contingency. Thus the project carries a minimum mission that achieves the science return deemed the minimum needed for mission success while increasing fuel

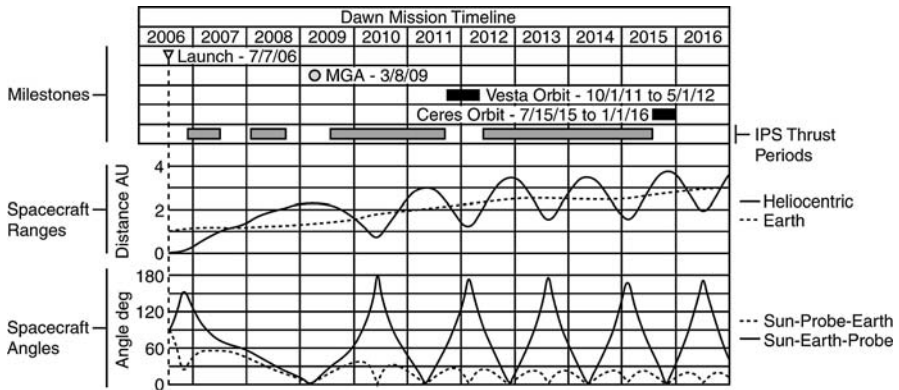


Fig. 12 Dawn mission timeline with milestones. Also shown are the spacecraft ranges, both heliocentric and geocentric, and the Sun-probe-Earth angle and the Sun-Earth-probe angle

reserves (or mass margin) and reducing operations costs. This mission, as illustrated in Fig. 13, arrives at Vesta in October 2011 as does the nominal or baseline mission but leaves Vesta earlier, in February 2012. It arrives at Ceres in September 2015 a month after the nominal mission. The end of mission is on the same date under both scenarios and is driven by cost considerations. Choice of the nominal mission or the minimum mission is not a binary decision. There is a continuum of possibilities. Moreover, it may be possible to arrive at Vesta earlier than October 2011 if all goes well. An ion propulsion system allows great flexibility in mission design.

9 Orbital Operations

When the Dawn spacecraft reaches either Vesta or Ceres it is moving slowly relative to the target body and can enter polar orbit around the target without any critical maneuvers or any use of hydrazine. Figure 14 illustrates the time line for Vesta operation.

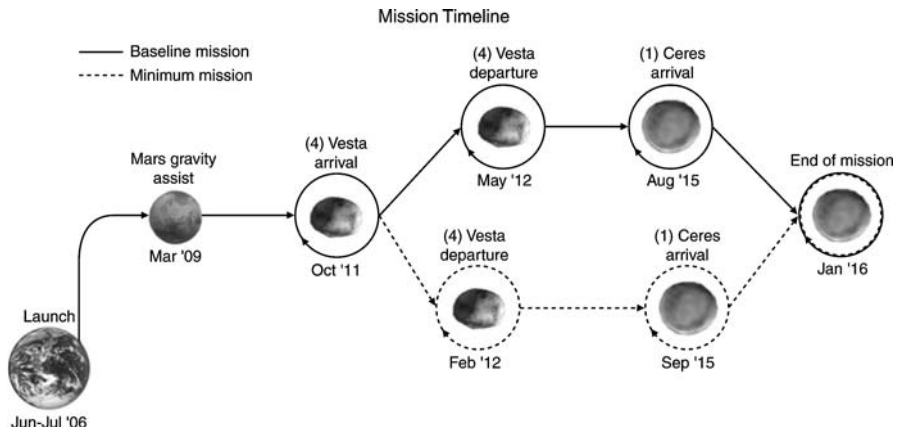


Fig. 13 Mission timeline showing the dates for the nominal mission and the minimum mission. The minimum mission allows more time for the interplanetary trajectory at the expense of data taking at Vesta and Ceres. This allows for less power or less fuel availability and provides more robust margins. Selection of the nominal or minimum mission is not a binary decision

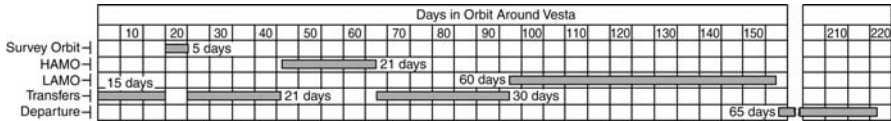


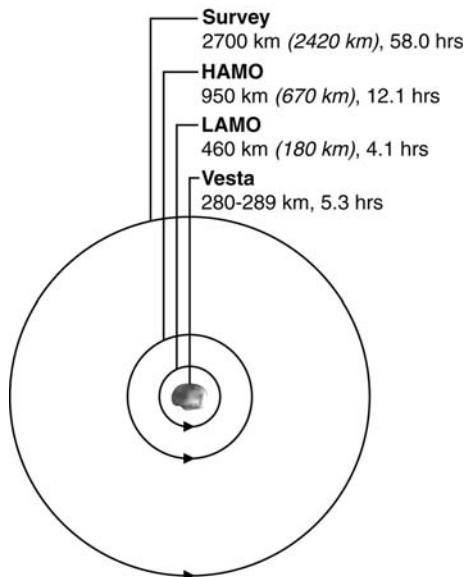
Fig. 14 Mission timeline showing orbital operations at Vesta

After a 15-day transfer trajectory, the spacecraft spends 5 days in a survey orbit where a complete set of images is taken as well as complete VIR mapping at low spatial resolution. A search of the region around Vesta for moons and debris is also carried out. Twenty-one days of thrusting carries Dawn to the high altitude-mapping orbit, HAMO, where the major portion of the framing camera imagery is obtained including that needed for topography. VIR obtains its highest spatial resolution over a limited portion of the surface. Then after an orbit transfer of 30 days the spacecraft reaches the low altitude mapping orbit or LAMO where the GRaND instrument obtains its prime gamma ray and neutron measurements over a period of 60 days, and precise tracking data are obtained for deriving the high-resolution gravity field. The LAMO orbit operations are nadir-pointed for GRAND with daily 4-hour tracks for gravity. High-resolution images and spectra may also be possible during LAMO. The ion thrusters are used to raise the spacecraft, with a few short stops to get critical observations under different lighting conditions. Figure 15 shows the three orbits to scale and gives the orbital periods to provide another perspective on the measurements.

A typical operations scenario is shown schematically in Fig. 16 for the survey orbit, showing Vesta at the center, with semi-circular arcs arranged in arcs that represent separate activity during the orbit.

The innermost circular band above the surface of Vesta shows when orbit maintenance and navigation (photo ops) pictures are taken. Much of this occurs over the nightside of Vesta with a few short photo ops on the lit side. The spacecraft does not enter Vesta’s shadow in any part of its orbit, nor are there Earth occultations. This policy prevents power

Fig. 15 Comparison of the three data taking orbits at Vesta, with orbits drawn to scale. Listed are radius (altitude) and period of the three orbits, and the equatorial radii and rotational period of Vesta



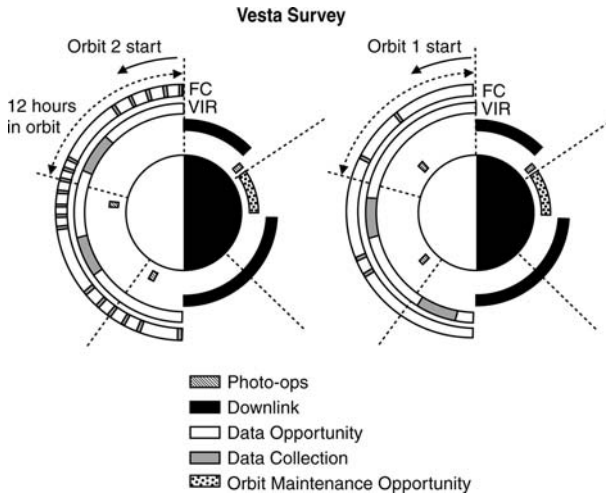


Fig. 16 Operations during the Vesta survey orbit

blackouts and thermal extremes in the case of solar occultations, and communication blackouts in the case of Earth occultations. The next set of circular arcs indicate where data are transmitted to Earth. Downlink time is reserved for the period when the spacecraft is over the darkside of the body, thus minimizing possible conflicts in pointing requirements between telemetry and science acquisition. The next set of arcs show the data collection opportunity for VIR on the lit side, with representative data collection periods shown to illustrate the amount of data that can be stored and telemetered during an orbit. The outer short arcs mark the data collection for the framing camera. There are only two survey orbits planned.

Figure 17 repeats the operations scenario for the HAMO orbit. Again photo opportunities, orbit maintenance, and downlink are restricted as much as possible to the period in which the spacecraft is above the dark side of Vesta, however the 8 hr downlink pass of necessity spills onto the lit side. HAMO is the prime observing period for the Framing Camera and images will be obtained at nadir in the clear filter and all seven color filters. In addition the spacecraft will be tilted off nadir to obtain stereo images suitable for topography. The amount of VIR data collected in a HAMO is limited by the data downlink bandwidth.

The operations planned for Ceres are similar to those planned for Vesta accounting for the different orbital periods shown in Fig. 18.

10 Closing Remarks

The objective of the Dawn mission is to enhance our understanding of Vesta and Ceres and through them derive a deeper understanding of the early solar system. We have learned much from meteorites and from telescopic observations of these asteroids and this process must continue. Dawn does not supplant the need to undertake cosmochemical studies of the HED meteorites nor the telescopic observation of Vesta and Ceres. Until Dawn reaches Vesta and Ceres, telescopic remote sensing will be essential to preparing us for the environment in which the mission must be conducted. And never will the mineralogical

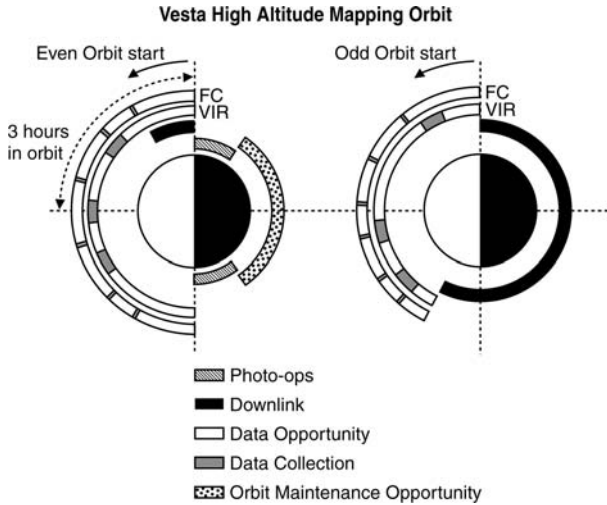
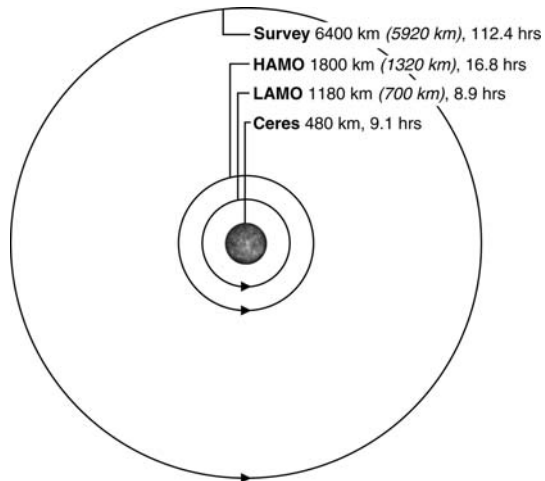


Fig. 17 Operations during the Vesta high altitude mapping orbit HAMO

Fig. 18 Comparison of the three data taking orbits for Ceres with orbits drawn to scale. Listed are orbit radius (altitude) and period of the three orbits, and the equatorial radius and the rotational period of Ceres



and elemental data from Dawn reach the level of accuracy possible from meteorites. Dawn’s role is to put these data into their proper geological context. We already have experienced the synergy between Dawn and the ground-based observers and the meteoriticists before the mission is even off the ground, as the mission’s development has focused interest on these two bodies. We strongly urge continued focus on the HED meteorites and HST and adaptive optic measurements of Vesta and Ceres at every opportunity until Dawn’s resolution clearly exceeds that of the 1 AU observations.

Finally, we emphasize that the Dawn mission is open to collaborative investigations of many types. Moreover, an open competition is planned to add participating scientists to Dawn, and to select guest investigators to analyze the archive of data that Dawn will bring to the Planetary Data System. We expect that these two avenues will enable many of those

who have interest in Vesta and Ceres, but no formal connection at present, to become partners in this exploratory program.

Acknowledgments A mission such as Dawn is the culmination of the work of many individuals and many organizations. We are extremely grateful to NASA for continuing to fund Dawn despite continued budgetary stress within the Discovery program. We also thank the German Space Agency, DLR, and the Italian Space Agency, ASI, for living by their commitments to fund their Dawn instruments at times of great stress within their own space programs. In the case of the German Framing Camera an additional strong commitment by the Max Planck Society was essential for the implementation of this investigation. Dawn has also benefited from strong support from its major partners in the US, Orbital Sciences Corporation, and the Jet Propulsion Laboratory. Some of the heroes of the Dawn program include Tom Frascchetti, John McCarthy, Valerie Thomas, Ann Grandfield, Marc Rayman, Joe Makowski, Ed Miller and Mike Violet among many, many others. The funding for the Dawn project in the US comes from the National Aeronautics and Space Administration and is administered by the Jet Propulsion Laboratory.

References

- M.F. A'Hearn, P.D. Feldman, *Icarus* **98**, 54–60 (1992)
 E. Asphaug, *Meteorit. Planet. Sci.* **32**, 965 (1997)
 R.P. Binzel, S. Xu, S.J. Bus, M.F. Skrutskie, M.R. Meyer, P. Knezek, E.S. Barker, *Science* **260**, 186 (1993)
 R.P. Binzel, M.J. Gaffey, P.C. Thomas, B.H. Zellner, A.D. Storrs, E.N. Wells, *Icarus* **128**, 95–103 (1997)
 T.H. Burbine, P.C. Buchanan, R.P. Binzel, S.J. Bus, T. Hiroi, J.L. Hinrichs, A. Meibom, T.J. McCoy, *Meteorit. Planet. Sci.* **36**, 761 (2001)
 W.M. Calvin, R.N. Clark, *Icarus* **104**, 69–78 (1993)
 A. Coradini et al., *Planet. Space. Sci.* **46**(9/10), 1291–1304 (1998)
 G. Dreibus, J. Bruckner, H. Wanke, *Meteorit. Planet. Sci.* **32**, A36 (1997)
 J.D. Drummond, R.Q. Fugate, J.C. Christou, *Icarus* **132**, 80–99 (1998)
 F. Fanale, J. Salvail, *Icarus* **82**, 97–110 (1989)
 M. Feierberg, M.J. Drake, *Science* **209**, 805–807 (1980)
 M. Feierberg, H.P. Larson, U. Fink, H.A. Smith, *Geochim. Cosmochim. Acta* **44**, 513–524 (1980)
 M.J. Gaffey, *Icarus* **127**, 130–157 (1997)
 M. Gaffey, T.B. McCord, *Space Sci. Rev.* **21**, 555–628 (1978)
 A. Ghosh, H.Y. McSween Jr., *Icarus* **134**, 187–206 (1998)
 L.F. Golubeva, D.I. Shestopalov, *Astronom. Vestnik* **29**, 37–46 (1995)
 S. Hasegawa, K. Murakawa, M. Ishiguro, H. Nonaka, N. Takato, C. Davis, M. Ueno, T. Hiroi, *Geophys. Res. Lett.* **30** (2003) DOI 10.1029/2003GL018627
 J.L. Hilton, *Astron. J.* **17**, 1077–1086 (1999)
 R.H. Hewins, H.E. Newsom, in *Meteorites and the Early Solar System*, eds. by J.F. Kerridge, M.S. Matthews (University of Arizona Press, Tucson, 1988), pp. 73–101
 S.B. Jacobsen, *Science* **300**, 1513–1514 (2003)
 M.S. Kelley, F. Vilas, M.J. Gaffey, P.A. Abell, *Icarus* **165**, 215–218 (2003)
 T.V.V. King, R.N. Clark, W.M. Calvin, D.M. Sherman, R.H. Brown, *Science* **255**, 1551–1553 (1992)
 T. Kleine, C. Munker, K. Mezger, H. Palme, *Nature* **418**, 952–955 (2002)
 A.S. Konopliv, J.K. Miller, W.M. Owen, D.K. Yeomans, J.D. Giorgini, R. Garmier, J.P. Barriot, *Icarus* **160**, 289–299 (2002)
 L.A. Lebofsky, M.A. Feierberg, A.T. Tokunaga, H.P. Larson, J.R. Johnson, *Icarus* **48**, 453–459 (1981)
 J.Y. Li, L.A. McFadden, J. Parker, Wm, E.F. Young, S.A. Stern, P.C. Thomas, C.T. Russell, M.V. Sykes, *Icarus* **182**, 143–160 (2006)
 G.W. Lugmair, A. Shukolyukov, *J. Geochim. Cosmochim. Acta.* **62**, 2863–2886 (1998)
 F. Marzari, A. Cellino, D.R. Davis, P. Farinella, V. Zappala, V. Vanzani, *Astron. Astrophys.* **316**, 248 (1996)
 T.B. McCord, C. Sotin, *J. Geophys. Res.* **110**, E05009 (2005)
 T.B. McCord, J.B. Adams, T.V. Johnson, *Science* **168**, 1445–1447 (1970)
 L.A. McFadden, T.B. McCord, C. Peters, *Icarus* **31**, 439–446 (1977)
 G. Michalak, *Astron. Astrophys.* **360**, 363–374 (2000)
 J.K. Miller, B.G. Williams, W.E. Bollman, R.P. Davis, C.E. Helfrich, D.J. Scheeres, S.P. Synnott, T.C. Wang, D.K. Yeomans, *J. Astro. S.* **43**, 453–476 (1995)
 F. Migliorini, A. Morbidelli, V. Zappala, B.J. Gladman, M.E. Bailey, A. Cellino, *Meteorit. Planet. Sci.* **32**, 903 (1997)

- L.E. Nyquist, D. Bogard, H. Takeda, B. Bansal, H. Wiesmann, C.Y. Shih, *Geochim. Cosmochim. Acta.* **61**, 2119–2138 (1997)
- T.H. Prettyman, W.C. Feldman, K.R. Fuller, S.A. Storms, S.A. Soldner, Cs. Szeles, F.P. Ameduri, D.J. Lawrence, M.C. Browne, C.E. Moss, *IEEE Trans. Nucl. Sci.* **49**, 1881–1886 (2002)
- T.H. Prettyman, W.C. Feldman, F.P. Ameduri, B.L. Barraclough, E.W. Cascio, K.R. Fuller, H.O. Funsten, D.J. Lawrence, G.W. McKinney, C.T. Russell, S.A. Soldner, S.A. Storms, Cs. Szeles, R.L. Tokar, *IEEE Trans. Nucl. Sci.* **50**, 1190–1197 (2003)
- M.D. Rayman, T.C. Fraschetti, C.A. Raymond, C.T. Russell, *Acta Astronautica* **58**, 605–616 (2006)
- F. Reininger et al., *SPIE* **2819**, 66–77 (1996)
- K. Righter, M.J. Drake, *Meteorit. Planet. Sci.* **32**, 929–944 (1997)
- A. Ruzicka, G.A. Snyder, L.A. Taylor, *Meteorit. Planet. Sci.* **32**, 825–840 (1997)
- E.N. Slyuta, S.A. Voropaev, *Icarus* **129**, 401–414 (1997)
- G. Srinivasan, J.N. Goswami, N. Bhandari, *Science* **284**, 1348–1350 (1999)
- F. Tera, R.W. Carlson, N.Z. Boctor, *Geochim. Cosmochim. Acta.* **61**, 1713–1732 (1997)
- D. Tholen, M.A. Barucci, in *Asteroids II*, ed. by R.P. Binzel, T. Gehrels, M.S. Matthews (University of Arizona Press, Tucson, 1989), pp. 298–315
- P.C. Thomas, R.P. Binzel, M.J. Gaffey, A.D. Storrs, E.N. Wells, B.H. Zellner, *Science* **277**, 1492–1495 (1997a)
- P.C. Thomas, R.P. Binzel, M.J. Gaffey, B.H. Zellner, A.D. Storrs, E.N. Wells, *Icarus* **128**, 88–94 (1997b)
- P.C. Thomas, J.Wm. Parker, L.A. McFadden, C.T. Russell, S.A. Stern, M.V. Sykes, E.F. Young, *Nature* **437**, 224–226 (2005)
- A.H. Treiman, A. Lanzirotti, D. Xirouchakis, *Earth Planet Sci. Lett.* **219**, 189–199 (2004)
- Q. Yin, S.B. Jacobsen, K. Yamashita, J. Blichart-Trott, P. Telouk, F. Albarede, *Nature* **418**, 949–952 (2002)
- F. Vilas, A.L. Cochran, K.S. Jarvis, *Icarus* **147**, 119 (2000)
- J.G. Williams, in *Asteroids II*, ed. by R.P. Binzel, T. Gehrels, M.S. Matthews (University of Arizona Press, Tucson, 1989), pp. 1034
- V. Zappala, A. Cellino, P. Farinella, Z. Knezevic, *Nature* **412**, 220–227 (1990)
- M.T. Zuber, D.E. Smith, F.G. Lemoine, G.A. Neumann, *Science* **266**, 1839–1843 (1994)
- M.T. Zuber, S.C. Solomon, R.J. Phillips, D.E. Smith, G.L. Tyler, O. Aharonson, G. Balmino, W.B. Banerdt, J.W. Head, F.G. Lemoine, P.J. McGovern, G.A. Neumann, D.D. Rowlands, *Science* **287**, 1788–1793 (2000)